Nonperturbative study of hadronization with heavy sources: The screening length as a function of the quark mass in the Schwinger model

J. Potvin
Department of Physics, University of Colorado, Boulder, Colorado 80309
(Received 12 April 1985)

We discuss the dynamical quark-mass dependence of the screening length (L_0), the distance at which the interaction between two (heavy) quarks begins to be screened as a result of pair production. We compute L_0 in the one-flavored massive Schwinger model in the continuum limit of its lattice formulation. The results of our numerical simulation (ensemble projector Monte Carlo) are shown to follow closely the lower bound $eL_0 \geq [\pi/16+(m/e)^2]^{1/2}$/(string tension), in which most of the quark-mass dependence is contained in the hadronic mass of the numerator. The vacuum expectation values of the electric field and the fermion occupation number have also been computed, showing directly the hadronization process. Finally, we apply those ideas in estimating the screening length in charmonium and Υ systems.

I. INTRODUCTION

According to the confinement hypothesis, two outgoing quarks will see their interaction screened by quark-pair creation, as their separation reaches a certain critical length L_0. The outcome will be such that, far beyond L_0, each quark and their respective cloud of dynamical pairs will form two (or more) distinct hadrons.[1]

The exact definition of the screening length L_0 is process and formalism dependent. Quark-pair production is stochastic in nature (it is a quantum effect); one appropriate quantity could be the pair production probability per unit length or separation (dP/dL). For example, in the *phenomenological* approaches to quark jet fragmentation such as the Lund model,[1,2] one uses Monte Carlo techniques to generate pairs and subsequently to form hadrons. There, dP/dL depends on the flavor of the created pairs, the energy available, the spatial extent of the gluon background, etc. Presumably, one could get some kind of "average" or "statistical" screening length by integrating dP/dL. In one of the simple Lund models,[3] such an L_0 gets smaller as hadronization proceeds further in time, because there is less kinetic energy available, as well as less background color to be screened.

The calculation of the screening length from first principles, i.e., from QCD, is a task that cannot be approached by perturbation theory, the latter being valid only for length scales much smaller than L_0. In this paper, we would like to use instead the lattice approach,[4,5] which has been shown to be quite successful in the investigation of nonperturbative aspects such as glueballs and the string tension.[6]

The state vectors in lattice QCD are eigenstates of the fermion and gauge fields, and therefore do not carry the degrees of freedom of individual quarks and gluons. Screening phenomena are usually studied by computing the interaction energy of a system of static color field sources, for various source separations.[7–9] Physically, such a calculation would correspond to situations involving heavy quarks (the sources), surrounded by gluons (the color gauge field), and light quarks (the dynamical fermions). Here the field sources are at rest; in doing so one is assuming some sort of adiabatic or Born-Oppenheimer approximation,[10] valid when the (slow) movement of the heavy quarks does not disturb the state of the gluons and light quarks. In that context, the screening length L_0 is defined as the heavy-quark separation for which the energy of the whole system is equal to the hadronic mass(es) one wishes to produce.[11]

Unfortunately, we are still waiting for a fast algorithm that will include dynamical quarks on the lattice. Progress is being made, however,[12] both in hardware and software; realistic calculations with light quarks should be within reach in a few years.

In the meantime, there are a few aspects of the screening-length calculation that could be studied with *simpler* lattice gauge theories. The benefits of such research would be to gain some insight about the screening mechanism, as well as developing efficient ways of computing L_0. There have been a few studies done along those lines already, by Bernard,[7] Dosch and Müller,[8] and DeGrand[9] in strong-coupling lattice QCD, and by many others on the continuum[13–17] as well as on the lattice Schwinger model.[18–20]

Screening by the dynamical fermion fields can be seen easily in lattice QCD at strong coupling (i.e., coarse lattice).[8,9] This effect arises when one computes the interaction energy, or the potential $V(L)$, of two sources in the fundamental representation of SU(3). The small-separation (L) behavior of $V(L)$ is dominated by the gluon part of the interaction and is given by

$$V=TL \ ,$$

where T is the string tension. At large separation however, the contribution of the dynamical fermions (here of mass m) balances the gluon interaction (screening), in which case we have

$$V=2m \ ,$$

i.e., an L-independent potential. In that example, the

 ©1985 The American Physical Society

screening length would be of that order

$$L_0 \approx \frac{2m}{T} . \tag{1.1}$$

Interestingly enough, quark-pair creation is not the only mechanism leading to screening. Bernard[7] has shown that, in *pure* lattice SU(2) theory, the potential between two sources in the adjoint representation of SU(2) can indeed be screened by gluons only.[7,9] Using Monte Carlo techniques, Bernard was able to demonstrate the existence of this mechanism near the continuum limit, and to evaluate the screening length as

$$L_0 \approx \frac{2m_g}{T_{\text{adj}}} \tag{1.2}$$

with m_g being the physical mass of a "constituent gluon" (500—800 MeV). T_{adj} is the "adjoint" string tension and is $\frac{8}{3}$ times larger than the "fundamental" string tension.[21]

Besides the investigation of the various screening mechanisms, there are other aspects worth studying. Among them is the question of the screening-length dependence on the number of quark flavors, or even the number of gluons. In this paper, however, we would like to concentrate our attention on the mass dependence of L_0, in the one-flavor massive Schwinger model.

The Schwinger model is quantum electrodynamics in one space and one time dimension (QED_2). Due to the absence of the two other space dimensions, static sources (or charges) can be *completely* screened as a result of fermion pair production. Moreover, this gauge theory is Abelian and also has no transverse photon; there will be no processes equivalent to gluon screening of adjoint sources.

Total charge screening in the continuum has been shown to occur in the case of massless dynamical fermions, by Schwinger,[14] Lowenstein and Swieca,[14] and Casher, Kogut, and Susskind[15] ($L_0 \approx \sqrt{\pi}/e$). Screening also operates in the massive case (Coleman, Jackiw, and Susskind[16]) but quantitative statements on L_0 for arbitrary masses are nonexistent, since the model cannot be, or has not been, solved exactly [there is a semiclassical study of the very massive case by Rothe, Rothe, and Swieca;[17] their L_0 is proportional to the (renormalized) fermion mass].

There are a few lattice studies of the potential $V(L)$ in massive QED_2, by Ranft and Schiller,[18] by Bender, Rothe, and Rothe,[19] and by Duncan and Furman (two flavors).[20] None of them were concerned with the systematic investigation of L_0's quark mass dependence as done, here, in this work.

To summarize our results, we have computed L_0 for large *and* small dynamical quark masses (m). The definition of the screening length, plus certain fairly natural assumptions about the mass and length dependence of the "string tension" $T_{(L)} \equiv V_{(L)}/e^2 L$, imply the lower bound

$$eL_0 \geq \frac{m_D}{eT_{(0)}} \approx \frac{2m_D}{e} . \tag{1.3}$$

$T_{(0)}$ is the (dimensionless) string tension for small L, and m_D the binding energy of the dynamical quark to the source. m_D has also been computed and found to be well approximated by

$$\frac{m_D}{e} \approx [\pi/16 + (m/e)^2]^{1/2} \tag{1.4}$$

so that

$$eL_0 \geq 2[\pi/16 + (m/e)^2]^{1/2} . \tag{1.5}$$

The data follow closely this last inequality and we conclude that most of the L_0's m dependence is contained in the binding energy m_D.

We have also calculated the expectation values of the electric field and fermion occupation number, showing hadronization and screening quite clearly.

Our study of screening will be done in the continuum limit of the lattice Hamiltonian formulation of QED_2 (Refs. 4 and 18). Quantitative results are obtained by using the ensemble projector Monte Carlo (EPMC) algorithm[22,23] which is only one of several Hamiltonian Monte Carlo algorithms in use in physics.[24–27]

The paper will be organized as follows. In Secs. II and III we review the continuum and lattice Schwinger models, and mention some known results that will be relevant to us. In Sec. IV we explain how we define and compute the screening length. Section V is a brief exposé of the EPMC algorithm as well as a detailed discussion of our systematics control. The Monte Carlo data are presented and discussed in Sec. VI. Finally, we elaborate in Sec. VII on future work and speculate about the screening length L_0 in charmonium and Υ systems.

II. CONTINUUM QED_2

The Schwinger model is defined by a Lagrangian identical in form to the four-dimensional QED Lagrangian, except for the fact that there are no Y or Z directions. Consequently, only one space integration is required—along the x axis; this in turn implies that the gauge field A is dimensionless (here $\hbar = c = 1$), while the condensate $\bar{\psi}\psi$ carries dimension of a mass. Moreover, the dynamical fermion's charge e as well as its mass m have also the dimension of a mass. The theory is therefore superrenormalizable, i.e., it requires no infinite renormalizations other than a redefinition of the zero energy density.

In the temporal gauge ($A^0 = 0$, $A^1 = A$), the model's Hamiltonian reads ($E = -\partial_t A$) (Ref. 13)

$$H_{\text{cont}} = \int dx \left[\frac{E^2}{2} - i\psi^\dagger \alpha (\partial_x + ieA)\psi + m\psi^\dagger \beta \psi \right] , \tag{2.1}$$

$$\beta = \begin{bmatrix} 1 & 0 \\ 0 & -1 \end{bmatrix} , \quad \alpha = \begin{bmatrix} 0 & 1 \\ 1 & 0 \end{bmatrix} .$$

In order to implement gauge invariance, the physical energy eigenstates must satisfy Gauss's law,

$$(\partial_x E - e\psi^\dagger \psi) \,|\, \text{PHY} \rangle = \rho_{(x)} \,|\, \text{PHY} \rangle . \tag{2.2}$$

The function $\rho_{(x)}$ is the eigenvalue of the operator on the left-hand side (LHS) of Eq. (2.2). When different from zero, $\rho_{(x)}$ represents a static, external charge or source located at x. Of course, when $\rho_{(x)} = 0$ for all x, the corresponding eigenstate with lowest energy will represent the

vacuum. In this work, we consider the cases where $\rho_{(x)}/e$ is an *integer*. The readers interested in the situations where $\rho_{(x)}/e \notin \mathbb{N}$ may consult Refs. 16 and 28.

A few remarks. Note that in practical calculations, Eqs. (2.1) and (2.2) have to be normal ordered. We will discuss this question in more detail in the section on the lattice Hamiltonian (Sec. III). Normal ordering in continuum QED_2 is discussed by Coleman.[28,29]

The theory based on the Hamiltonian (2.1) can be solved analytically only in the regimes $m \gg e$ and $m \ll e$ where, in fact, some analysis of its mass spectrum has been done.[28] Moreover, when $m=0$, one can compute exactly the interaction energy (the potential) between two sources of opposite charge e separated by the distance L (Ref. 13):

$$V(L)=\frac{e\sqrt{\pi}}{2}(1-e^{-eL/\sqrt{\pi}}) . \tag{2.3}$$

Note that

$$V(L)\approx\frac{e^2L}{2} \quad \text{when } L \ll \sqrt{\pi}/e \tag{2.4}$$

and

$$V(L)\approx\frac{e\sqrt{\pi}}{2} \quad \text{when } L \gg \sqrt{\pi}/e . \tag{2.5}$$

$V(L)$ exhibits linear behavior at small distance, while screening occurs at large distance [$V(L)\approx$constant]. All this can also be found in the case of very massive dynamical quarks (large m/e).[17]

With respect to confinement and screening, QED_2 is qualitatively closer to QCD_4 than to QED_4. For that reason, we hereafter adopt the following nomenclature. The dynamical fermions (ψ) will be called *d quarks*, while the static sources $\rho_{(x)}$ will carry the name of *c quarks* or *heavy quarks*. The field E will still be referred to as the *electric field*.

III. LATTICE QED_2

A fair amount of work has already been devoted to the study of the lattice Schwinger model. Most of that effort was geared toward the test of various formalisms (Euclidean, Hamiltonian, Monte Caro, Padé, etc.) by comparing with *known* continuum results. Let us mention the study of the mass gap,[20,30–34] chiral-symmetry breaking,[18,35] screening,[18–20] and miscellaneous aspects such as SLAC fermions and the method of finite elements.[36]

The lattice Hamiltonian for QED_2 is given by[18]

$$H_{\text{latt}}=\sum_{n=0}^{S-1}\left[\frac{(ea)^2}{2}E_n^{\,2}+(-)^n(am)\psi_n^\dagger\psi_n + \tfrac{1}{2}(\psi_n^\dagger e^{ieaA_n}\psi_{n+1}+\text{H.c.})\right] . \tag{3.1}$$

The lattice is a chain of S (even) sites; (anti)periodic boundary conditions are assumed and the lattice fermions are of the Kogut-Susskind type, i.e.,

$$\psi_n \leftrightarrow (i)^n\psi_{(x)}^{(\text{up})} , \quad x=na , \quad n \text{ even}$$
$$\psi_n \leftrightarrow (i)^n\psi_{(x)}^{(\text{down})} , \quad x=na , \quad n \text{ odd} .$$

The quantity a is the lattice spacing; the constants ea ($\equiv g$) and am ($\equiv\mu$) are dimensionless, as well as H_{latt}, E_n, and ψ_n. The (anti)commutation rules are given by

$$\{\psi_n^\dagger,\psi_m\}=\delta_{n,m} , \quad \{\psi_n,\psi_m\}=0 ,$$
$$[A_n,\psi_m]=0 , \quad [E_n,\psi_m]=0 , \tag{3.2}$$
$$[E_m,e^{\pm ieaA_n}]=\pm\delta_{n,m}e^{\pm ieaA_n} .$$

The Hamiltonian (3.1) is invariant with respect to space translations, i.e., translations by two sites; when $m=0$, H_{latt} is invariant with respect to (discrete) chiral transformation, i.e., translation by one site.[4]

Because of the commutators in (3.2), it is possible to find on each site a basis of state vectors that diagonalize simultaneously the operators E_n and $\psi_n^\dagger\psi_n$:

$$E_n \mid e_n,N_n\rangle = e_n \mid e_n,N_n\rangle , \quad e_n=0,\pm1,\ldots ,$$
$$\psi_n^\dagger\psi_n \mid e_n,N_n\rangle = N_n \mid e_n,N_n\rangle , \quad N_n=0,1$$

(a lattice state would be $\mid\{e_n,N_n\}\rangle=\prod_j\otimes\mid e_j,N_j\rangle$).

As in the continuum, "good" lattice states will have to satisfy Gauss's law on each site:

$$G_n \mid \text{latt}\rangle=\rho_n \mid \text{latt}\rangle ,$$
$$G_n=(E_n-E_{n-1})-(\psi_n^\dagger\psi_n-Q_n) , \tag{3.3}$$

where G_n is the generator of gauge transformations. The Q_n's are integers and correspond to the normal ordering of $\psi^\dagger\psi$ ($:\psi^\dagger\psi:$). Recall that, in the continuum,

$$:\psi_{(x)}^\dagger\psi_{(x)}:=\psi_{(x)}^{*\,(\text{up})}\psi_{(x)}^{(\text{up})}+\psi_{(x)}^{*\,(\text{down})}\psi_{(x)}^{(\text{down})}-\delta_{(0)} .$$

On the lattice, this expression would correspond to

$$\psi_n^\dagger\psi_n+\psi_{n+1}^\dagger\psi_{n+1}-1$$

so that

$$Q_n+Q_{n+1}=1 .$$

We choose to set

$$Q_n=0 \text{ for } n \text{ even} ,$$
$$Q_n=1 \text{ for } n \text{ odd} . \tag{3.4}$$

In plain words, this choice means that we are adding $S/2$ background (static) charges to the system, in order to neutralize the charge of the Dirac sea.

The continuum limit of the lattice model corresponding to (3.1) is defined by considering the physical quantities of interest (energies, lengths, etc.) in the regime (recall that $g=ae$ and $\mu=am$) (Refs. 18 and 30)

$$a\to0 , \quad g\to0, \quad \mu\to0$$
$$e,m \text{ fixed} \tag{3.5}$$

and

$$m/e=\text{constant} , \quad \mu/g=m/e .$$

Here e is independent of the cutoff a because QED_2 is super-renormalizable.

If we consider (dimensionless) lattice energies (ϵ), for example, we can write

$$\epsilon = aE_{\text{cont}} = g\frac{E_{\text{cont}}}{e} .$$

For large a (or g), ϵ will be a function of g and μ. In the continuum limit however, one would expect the continuum energy to be equal to ϵ/a, and be independent of the lattice spacing. In other words we should get scaling

$$\text{cont lim}\left[\frac{\epsilon}{g}\right] = \frac{E_{\text{cont}}}{e} = \text{constant, } a \text{ independent} . \quad (3.6)$$

Similarly, for (dimensionless) lengths (l) computed on the lattice we have

$$\text{cont lim}(gl) = eL_{\text{cont}} = \text{constant} . \quad (3.7)$$

Practically speaking, (3.6) and (3.7) will amount in computing ϵ and l for many small values of g and μ—typically $g \lesssim 0.5$ and $\mu \lesssim 1.0$—and fitting a straight line through the data plotted on ϵ vs g and l vs g^{-1} graphs. The slope of these lines should give the continuum results we are seeking. More on this in Sec. VI.

Before closing this section, let us derive a few results to be useful later.

In the limit of large g and μ, the Hamiltonian (3.1) is approximated by

$$H_{\text{latt}} \simeq H_0 \equiv \sum_{n=0}^{S-1}\left[\frac{g^2}{2}E_n^2 + (-)^n\mu\psi_n^\dagger\psi_n\right] . \quad (3.8)$$

It is seen immediately that the vectors $|e_n, N_n\rangle$ are eigenstates of H_0. Let

$$|0\rangle \equiv \prod_{k \text{ odd}}\psi_k^\dagger\left\{\prod_i \otimes re_i = 0 , \; N_i = 0\right\} ; \quad (3.9)$$

then, H_0 has the following eigenstates and eigenvalues.

The ground state ($\rho_n = 0$, all n):

$$|0\rangle; \epsilon_{\text{gs}} = -\frac{S}{2}\mu . \quad (3.10)$$

The lowest, one-charged state ($\rho_n = +\delta_{n,i}$, i is odd; the lattice then contains one source, and $S/2+1$ dynamical fermions):

$$(-)^P\psi_i|0\rangle , \quad \epsilon_{+1} = -\frac{S}{2}\mu + \mu . \quad (3.11)$$

The lowest, doubly-charged states ($\rho_n = \delta_{n,i} - \delta_{n,i+1}$, i and l are odd):

$$\text{"STRING"} \quad \prod_{j=i}^{i+l-1}(e^{iaeA_j})|0\rangle ; \quad \epsilon_l = -\frac{S}{2}\mu + \frac{g^2}{2}l , \quad (3.12)$$

$$\text{"TWO SOURCES"} \quad \psi_i\psi_{i+l}^\dagger|0\rangle ; \quad \epsilon_l = -\frac{S}{2}\mu + 2\mu . \quad (3.13)$$

Let us mention that the vacuum energy of the full Hamiltonian (3.1) has been evaluated with strong coupling expansions, up to order $1/g^{16}$ (Refs. 32 and 33). This result, plus a Padé-improved formula, can be found in Ref. 33.

Finally, when e and m are set to zero in (3.1), the resulting Hamiltonian is equivalent to an XY antiferromagnetic spin chain.[37] For long chains ($S \to \infty$), the ground-state energy is equal to $-S/\pi$.

IV. THE SCREENING LENGTH

A. Definition

There are two distinct length scales involved in screening phenomena. First, there is the length at which two outgoing c quarks have their interaction completely screened, each forming now two distinct hadrons. This length, called L_0^{hadron}, can be obtained in the lattice approach via the condition $V_{c\bar{c}}^{(L_0^{\text{hadron}})} = 2m_D$ (hadronization). Examples of L_0^{hadron} are given by Eqs. (1.1) and (1.2).

On the other hand there is also the $c\bar{c}$ separation for which the first few individual d-quark pairs pop out of the vacuum. This length, L_0^{pair}, is more important in formalisms based on perturbation theory.[1-3] Intuitively, we expect L_0^{pair} to be much smaller than L_0^{hadron}, especially in the limit of small m.

The definition of the screening length L_0 used in this work will combine information from both L_0^{pair} and L_0^{hadron}. It is given by

$$V_{c\bar{c}}^{(L_0)} = m_D . \quad (4.1)$$

Equation (4.1) is a compromise between L_0^{pair} and L_0^{hadron} because, (1) L_0 corresponds to an energy scale of the same order of magnitude as the energy involved in hadronization and (2) L_0 does not correspond to *complete* screening of the $c\bar{c}$ pair but nevertheless describes a situation where *a few* d-quark pairs have already been created (this should be true for $m/e \lesssim 1.00$, but not for $m \to \infty$ where only one pair is sufficient for complete screening).

B. Useful results

It is possible to derive L_0 from (4.1) in the two extreme cases $m = 0$ and $m \to \infty$.

In the massless case, we already have $V_{c\bar{c}}^{(L)}$ [see Eq. (2.3)]. When hadronization takes place at $L \gg \sqrt{\pi}/e$, we have $V_{c\bar{c}} = 2m_D$. From (2.5) then

$$\frac{m_D}{e} = \sqrt{\pi/16} , \quad (4.2)$$

which, included in Eq. (4.1) yields

$$\frac{e\sqrt{\pi}}{2}(1 - e^{-eL_0/\sqrt{\pi}}) = \left[\frac{e\sqrt{\pi}}{2}\right]\frac{1}{2}$$

or

$$eL_0 = -\sqrt{\pi}\ln(\tfrac{1}{2}) \approx 1.23 . \quad (4.3)$$

On the other hand, when $m/e \to \infty$, we can approximate H_{cont} [see Eq. (2.1)] by

$$H_{\text{cont}} \simeq \int dx\left[\frac{E^2}{2} + m\psi^\dagger\beta\psi\right] , \quad (4.4)$$

since $v = P - eA \simeq 0$ (nonrelativistic approximation). For $eL < 4m/e$, the potential should be

$$V_{c\bar{c}}^{(L)} = \frac{e^2}{2}L .$$

On the other hand, by applying the ideas of the nonrelativistic quark model, the binding energy of the d quark to the heavy one should be given by

$$\frac{m_D}{e}=\frac{m}{e}\ , \tag{4.5}$$

in which case (4.1) yields

$$eL_0=2\frac{m}{e}\ . \tag{4.6}$$

C. A lower bound

Let us define the "string tension" $T_{(L)}$ as

$$eLT_{(L)}\equiv\frac{1}{e}V_{c\bar{c}}^{(L)}\ . \tag{4.7}$$

This result in Eq. (4.1) yields

$$eL_0=\frac{m_D}{e}\left[\frac{1}{T_{(L_0)}}\right]\ . \tag{4.8}$$

In the cases $m=0$ and $m/e\to\infty$, one can show that $T_{(L=0)}\geq T_{(L)}$ for all L. If we assume such an inequality to be valid for arbitrary m/e, we get the lower bound

$$eL_0\geq\frac{m_D}{e}\frac{1}{T_{(0)}}\ . \tag{4.9}$$

Moreover, one can also check that $T_{(0)}=\frac{1}{2}$ for both $m=0$ and $m/e\to\infty$ cases; again, we assume this to be true for all m/e, so that

$$eL_0\geq 2\left[\frac{m_D}{e}\right]\ . \tag{4.10}$$

Inequality (4.9) gives us a systematic way of studying the m dependence of the screening length, by factorizing two possible sources: $T_{(0)}$ and m_D. More on this in Sec. VI.

V. THE ENSEMBLE PROJECTOR MONTE CARLO (EPMC) ALGORITHM

A. The method

Introduced by Campbell, DeGrand, and Mazumdar,[22] the EPMC algorithm is a faster and more accurate version[23] of the projector Monte Carlo algorithm of Blankenbecler and Sugar.[24]

The EPMC algorithm is based on the following theorem. Consider the Hamiltonian $H_{\rm latt}$ with ground state $|0\rangle$ and energy ϵ_0, and let

$$u=\exp(-tH_{\rm latt})\ , \tag{5.1}$$

where t is a positive real number. Suppose also that we have the states $|\phi\rangle$ and $|\psi^{(0)}\rangle$ such that

$$\langle\phi|0\rangle\neq 0\ ,\quad \langle\psi^{(0)}|0\rangle\neq 0\ .$$

Finally, let us define S_n as

$$S_n\equiv\frac{\langle\phi|u^n|\psi^{(0)}\rangle}{\langle\phi|u^{n-1}|\psi^{(0)}\rangle}\ . \tag{5.2}$$

Then, it follows that

$$\lim_{n\to\infty}S_n=e^{-t\epsilon_0}\ . \tag{5.3}$$

By virtue of (5.2) and (5.3), the EPMC algorithm will compute the vacuum state energy of the theory. Actually, it can do more. Because $H_{\rm latt}$ is gauge invariant, i.e., $[G_n,H_{\rm latt}]=0$ [see Eqs. (3.1) and (3.3)], the EPMC algorithm will compute to the lowest energy state of any set of vectors characterized by Eq. (3.3) with *given* ρ_n. In other words, it will be possible to obtain the lowest energy of any conceivable source distribution. This is a welcomed feature, since we need the lowest energy of states containing zero, one, and two c quarks.

The EPMC is a Monte Carlo algorithm; it has been described in detail in Ref. 23. In brief, it is constructed as follows.

The basic ingredient in an EPMC calculation is the vector $u|\psi\rangle$, written in a convenient basis (here it is $|\{e_n,N_n\}\rangle$)

$$u|\psi\rangle=\sum_{\{\bar{e}_n,\bar{N}_n\}}a^{\psi}_{\{e_n,N_n\}}\left[\sum_{\{\bar{e}_n,\bar{N}_n\}}\langle\{\bar{e}_n,\bar{N}_n\}|u|\{e_n,N_n\}\rangle|\{\bar{e}_n,\bar{N}_n\}\rangle\right]\ . \tag{5.4}$$

(In the computer memory, $|\psi\rangle$ corresponds to a *collection* of states $|\{e_n,N_n\}\rangle$, with copies made according to $|a^{\psi}|$.)

The expectation value $\langle\{\bar{e}_n,\bar{N}_n\}|u|\{e_n,N_n\}\rangle$ is difficult to evaluate in closed form. This is why we break up the Hamiltonian into two parts, $H_{\rm latt}=H_1+H_2$, and use the approximation

$$e^{-tH_{\rm latt}}\simeq e^{-tH_1}e^{-tH_2}+O(t^2)\ . \tag{5.5}$$

H_1 (H_2) is chosen to have the same form as $H_{\rm latt}$ in Eq. (3.1), except that the index n in the sum runs over the even (odd) sites only: this is the checkerboard pattern.

By inserting a complete set of states in between the two exponentials in (5.5), $\langle\{\bar{e}_n,\bar{N}_n\}|u|\{e_n,N_n\}\rangle$ then can be written as a sum, each term being a product of this type

$$\left[\prod_n^{\rm even}\langle e_n,N_n,N_{n+1}|e^{-th_1^{(n)}}|e'_n,N'_n,N'_{n+1}\rangle\right]\left[\prod_n^{\rm odd}\langle e'_n,N'_n,N'_{n+1}|e^{-th_2^{(n)}}|\bar{e}_n,\bar{N}_n,\bar{N}_{n+1}\rangle\right]$$

with

$$h_j^{(n)}=\frac{g^2}{2}E_n^{\,2}+(-)^{j-1}\mu\psi_n^\dagger\psi_n + \tfrac{1}{2}(\psi_n^\dagger e^{iea_n A_n}\psi_{n+1}+\text{H.c.});\ \ j=1,2\ , \tag{5.6}$$

i.e., a product involving matrix elements defined on *two* sites only. These $\langle e_n',N_n',N_{n+1}'\,|\,e^{-th_i^{(n)}}\,|\,e_n,N_n,N_{n+1}\rangle$ can be evaluated in a straightforward manner. We refer the reader to Schiller and Ranft[18] for more details, in particular their Table 1 which contains the worked out expressions (*our* results do not contain minus signs because we have made the change of variable $\psi_n\to(-)^n\psi_n$; also their α parameter should be set to zero).

At this point we rewrite the matrix element in terms of probabilities and scores, i.e. $(\alpha_n\leftrightarrow e_n,N_n,N_{n+1})$,

$$\langle\alpha_n'\,|\,e^{-th_i}\,|\,\hat{\alpha}_n\rangle\equiv P^{(i)}_{\alpha_n',\hat{\alpha}_n}S^{(i)}_{\alpha_n',\hat{\alpha}_n}\ ,\ \ \sum_{\alpha_n}P^{(i)}_{\alpha_n,\alpha_n'}=1\ .$$

The P's and the S's are otherwise arbitrary.[23] The most efficient choice turned out to be one similar to Campbell, DeGrand, and Mazumdar.[23] Let us distinguish four types of nonzero matrix elements:

TYPE A: $N_n'=N_{n+1}'=\hat{N}_n=\hat{N}_{n+1}=0$.

TYPE B: $N_n'=N_{n+1}'=\hat{N}_n=\hat{N}_{n+1}=1$.

TYPE C: $N_n'=1$ and $N_{n+1}'=0$;

$\hat{N}_n=1$, $\hat{N}_{n+1}=0$ and vice versa .

TYPE D: $N_n'=0$ and $N_{n+1}'=1$;

$\hat{N}_n=1$, $\hat{N}_{n+1}=0$ and vice versa .

Referring to the expressions shown in Schiller and Ranft,[18] Table 1, the score (S) will be given by the exponential containing the square of the electric flux; the probability will be given by the other factors (the quantity P will also contain some normalization factor that has to be included in S as well).

This choice of probability and score has the advantage that $P^{(i)}_{\alpha_n,\alpha_n'}$ is independent of the e_n's; one needs to store only 4×2 (transitions)$\times2$ (checkerboard)$=16$ numbers.

As shown in Ref. 23, the P's and S's are recombined in such a way that

$$u\,|\,\psi\rangle=\sum_{i,j}a_i^\psi\mathscr{P}_{ij}\mathscr{S}_{ij}\,|\,j\rangle\ .$$

With the overall probability $\mathscr{P}_{ij}$, one will generate a lattice configuration j (i.e., state $|\,\{e_nN_n\}\rangle$) from a starting state i. The number of copies of j will be determined by the overall scores $\mathscr{S}_{ij}$.

We choose $|\,\phi\rangle$ to be a broad state, i.e.,

$$|\,\phi\rangle=\sum_{\{e_n,N_n\}}|\,\{e_n,N_n\}\rangle$$

so that in the stochastic process outlined above, $\langle\phi\,|\,u\,|\,\psi\rangle$ is proportional to the number of state generated through $\mathscr{P}_{ij}$, plus their copies (in this work this amounts to about 3000—8000 states).

In order to find ϵ_0 through Eqs. (5.2) and (5.3), apply u to a given starting state $|\,\psi^{(0)}\rangle$; one gets a new ensemble, $|\,\psi^{(1)}\rangle$, on which u is applied again, and so on.

B. The starting state $|\,\psi^{(0)}\rangle$

In order to compute the screening length, one needs to find $V_{c\bar{c}}^{(L)}$ and m_D, or $v_{c\bar{c}}^{(l)}$ and $\mathscr{M}_D$ in lattice units. With the EPMC algorithm, we can calculate $\epsilon_0,\epsilon_{+1},\epsilon_{+1,-1}^{(l)}$ which correspond, respectively, to the lowest energy state containing 0 source (the vacuum), one c quark, and two c quarks of opposite charge. The relationship between those quantities is as follows:

$$\begin{aligned}&\mathscr{M}_D=\epsilon_{+1}-\epsilon_0\ ,\\ &v_{c\bar{c}}^{(l)}=\epsilon_{+1,-1}^{(l)}-\epsilon_0\ ,\\ &v_{c\bar{c}}^{(l)}-\mathscr{M}_D=\epsilon_{+1,-1}^{(l)}-\epsilon_{+1}\ .\end{aligned}\tag{5.7}$$

Note the following remarkable cases:

$$\begin{aligned}&l=0\to\epsilon_{+1,-1}^{(0)}-\epsilon_{+1}=-\mathscr{M}_D\ ,\\ &l=\infty\to\epsilon_{+1,-1}^{(\infty)}-\epsilon_{+1}=+\mathscr{M}_D\ (\text{since } v_{c\bar{c}}^{(\infty)}=2\mathscr{M}_D)\ ,\\ &l=l_0\to\epsilon_{+1,-1}^{(l_0)}-\epsilon_{+1}=0\ .\end{aligned}\tag{5.8}$$

The starting states $|\,\psi^{(0)}\rangle$ have been chosen so that they are eigenstates of H_{latt} in the strong-coupling limit [see Eq. (3.8)] and satisfy Gauss's law. They are the ones listed in Eqs. (3.10)—(3.13). In principle, they should be invariant with respect to translations (by two sites) since we are computing *masses*. Equation (3.10) certainly has this invariance, but not (3.11) and (3.12); this is of no consequence however. The reason is that, since H_{latt} is gauge invariant, the static sources will not move on the lattice upon any application of H. Moreover, because we have used (anti)periodic boundary conditions, the expectation values of H will not change upon moving "by hand" the position of the sources, keeping their relative separation, number, and charge constant.

Note that in the case $\mu=0$ where H_{latt} is invariant under translation by one site (chiral transformation), the state $|\,0\rangle$ itself is not. This is a statement of dynamical chiral symmetry breaking. There is *only one* state characterized by $\rho_n=0$ (all n) which minimizes the ground-state energy of H_0.

C. Systematics control

Let us review the two possible sources of systematic errors. These have been investigated by comparing the EPMC data with known facts, such as (2.3), (4.3), and (3.8)—(3.13). Moreover we checked that $\epsilon_0=-S/\pi$ when g and $\mu\to0$ (Ref. 37).

1. Finite lattice size

We have used (anti)periodic boundary conditions, on lattices of length S (even). Even if (anti)periodic boundary conditions are known to minimize size effects, we still have to make sure that S is much larger than the length scale of the physics one is studying.

It appears that the algorithm works best in the coupling

range $0.1 \leq g \leq 1.5$. In order to estimate a good lattice length for that interval, we have interpolated between two known values of the screening length in the continuum [see Eqs. (4.3) and (4.6)]:

$$gl_0 \approx 1.23 \ , \ \mu/g = 0 \ ,$$
$$gl_0 \approx 2\mu/g \ , \ \mu/g \to \infty \ . \tag{5.9}$$

Typical screening lengths would then be

$$g = 0.2 \to l_0 = \begin{cases} 6 & \text{if } \mu/g = 0 \ , \\ 30 & \text{if } \mu/g = 3 \ , \end{cases}$$
$$g = 0.7 \to l_0 = \begin{cases} 1.7 & \text{if } \mu/g = 0 \ , \\ 8.5 & \text{if } \mu/g = 3 \ . \end{cases}$$

Consequently, a lattice of length 30 should be large enough to contain all the relevant physics for $0 \leq \mu/g \leq 0.6$ with $0.1 \leq g \leq 1.5$, and $\mu/g \approx 3$ with $g \approx 1$.

To check the absence of size effects in our data, we have made a few calculations with lattices of length 22 ($\mu/g = 0$, 0.4, 0.6, 3 and $g = 0.3$–0.5). No such effect has been seen.

2. *t systematics*

By definition [Eqs. (5.1)–(5.3)], the EPMC algorithm introduces an extra parameter t. From our choice of probability $P^{(i)}_{\alpha_n, \alpha_n'}$, there will be more fluctuations (i.e., transitions of types C and D) with higher t. On the other hand, if t is too small, no transition will occur; $|\psi^{(n)}\rangle \simeq |\psi^{(0)}\rangle$. If t is too large, it will take a very large number of states in the ensemble $|\psi^{(n)}\rangle$ in order to get any results. If t is too small, it will require too many applications of the projector u. We believe that the best values which avoid these two complications are contained in the range $0.1 \leq t \leq 0.7$, for which about 3000–8000 lattice configurations were contained in any ensemble $|\psi^{(n)}\rangle$. The total number of projector applications was 100–150.

We have computed energies for different values of t in the above interval. For the cases $\mu/g = 0$, 0.1, 0.6, 3, we have noticed no systematics at all. However, in the case $0.3 \leq \mu/g \leq 0.5$, the energies were t independent in the range $0.45 \leq t \leq 0.7$ only. Our explanation is that, in terms of strong coupling expansion, $0.3 \leq \mu/g \leq 0.5$ is a range where the high-order terms in $(1/g^2)^n$ are enhanced by factors such as[33]

$$\frac{10(1+\mu)}{(1+2\mu)^5(3+2\mu)}$$

or

$$\frac{10^3(1+10\mu)}{(1+2\mu)^7(3+2\mu)^2(1+\mu)} \ .$$

In the language of the EPMC algorithm, this means that one needs more fluctuations, i.e., higher t.

3. *Scaling regime*

From the work of a few investigators[19,30] in the case $m/e = 0$, the value of g below which one observes scaling is $g_s \approx 0.4$. Our calculations confirm this also, as we will see in Sec. VI.

On the other hand, the continuum Hamiltonian corresponding to $m/e \to \infty$ is given by (4.4). This translates on the lattice into H_0 [Eq. (3.8)], which is easily solved. Equations (3.9)–(3.13), together with (5.7), yield

$$\frac{\mathcal{M}_D}{g} = \frac{\mu}{g} = \frac{m}{e}$$

and

$$gl_0 = 2\frac{\mu}{g} = \frac{2m}{e} \ ,$$

i.e., the quantities $\mathcal{M}_D/g$ and gl_0 scale for *all* values of g. From this we conclude that $g_s = \infty$.

By interpolating between those two results we conclude tentatively that g_s should increase with m/e. Unfortunately, we do not know quantitatively what this increase is. Therefore, we have chosen to set

$$g_s \approx 0.4 \text{ for } m/e = 0, 0.1, 0.4, 0.6 \ ,$$
$$g_s \approx 1 \text{ for } m/e = 3 \ . \tag{5.10}$$

About 400 CPU hours on a Vax 11/780 were needed to generate the data reported in this work.

VI. NUMERICAL RESULTS

A. The screening length

According to (5.7), one needs to compute ϵ_0, ϵ_{+1}, and $\epsilon^{(l)}_{+1,-1}$ as defined in Sec. V B. To measure the screening length, we use Eqs. (5.8) and compute $\epsilon^{(l)}_{+1,-1}$ for three or four values of l, as suggested by (5.9). l_0 was estimated by interpolating where the data were expected to cross the zero line, on a $\epsilon^{(l)}_{+1,-1} - \epsilon_{+1}$ versus l plot.

The continuum limit numbers shown in Table I were extracted from the Monte Carlo simulation by using Eqs. (3.6), (3.7), and (5.10). We see good agreement with the exact results (numbers in parentheses), except maybe for L_0 at $m = 0$, where the simulation yielded a value a bit high but well within a 2σ-deviation notwithstanding.

Scaling is clearly seen in the calculation of $\mathcal{M}_D$ and l_0, as shown in Figs. 1 and 4. On the other hand, screening shows up rather nicely in $v^{(l)}_{c\bar{c}}$ (Fig. 2), while hadronization is observed in Fig. 3, on a $\epsilon^{(l)}_{+1,-1} - \epsilon_{+1}$ plot [compare with (5.8)]. To summarize the data of Table I, we have Figs. 5 and 6, which are m_D/e vs m/e, and $L_0 e$ vs m/e plots.

TABLE I. Calculated continuum values for the binding energy m_D/e and the screening length $L_0 e$. The numbers in parentheses are exact results.

m/e	m_D/e	eL_0
0	0.43±0.05 (0.44)	1.62±0.25 (1.23)
0.1	0.47±0.03	
0.4	0.69±0.05	2.00±0.21
0.6	0.89±0.08	2.27±0.17
3.0	3.11±0.22 (3.00)	5.97±0.60 (6.00)

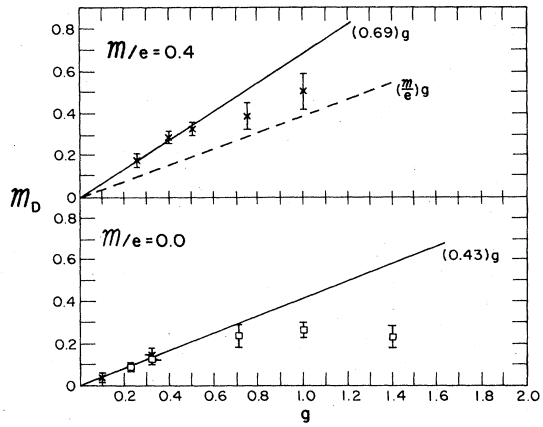

FIG. 1. The binding energy $\mathcal{M}_D$ (in lattice units) versus the coupling constant, for two values of the d-quark mass. Crosses and boxes represent data calculated on lattices of length 30 and 22, respectively.

In Fig. 5 we compare the data with the following *assumed* interpolating curve:

$$\frac{m_D}{e}=[\pi/16+(m/e)^2]^{1/2}\ . \tag{6.1}$$

Equation (6.1) is seen to be closely followed by the data. Recall that in our model, the mass of the c quark (m_c) is infinite so, in reality, m_D/e is the *binding* energy of the d-quark "cloud" to the c quark. In fact, if M_D is the mass of the hadron, we would have

$$\frac{M_D}{e}=(m_D+m_c)\frac{1}{e}=\frac{m_c}{e}+[\pi/16+(m/e)^2]^{1/2}\ . \tag{6.2}$$

This expression is reminiscent of the MIT bag model,[38] which describes hadrons as cavities enclosing (quasi)free quarks. In the case corresponding to (6.2), the hadron would be made of one flavor of light, relativistic quark and one flavor of static heavy quark.

On the basis of the close agreement between the data and (6.1), we use the latter in the lower bound (4.10) and

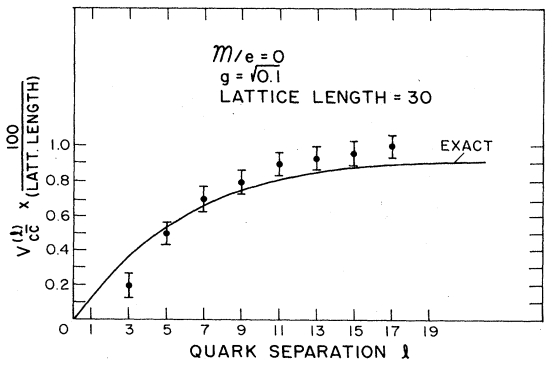

FIG. 2. The heavy quark potential $v_{c\bar{c}}^{(l)}$ (in lattice units) as a function of the separation l. The continuous line represents the exact answer [Eq. (2.3)].

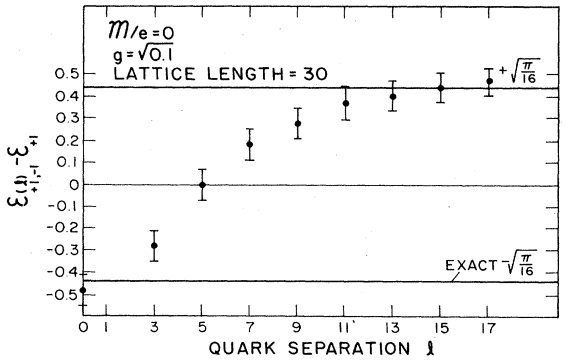

FIG. 3. The energy difference $\epsilon_{+1-1}^{(l)}-\epsilon_{+1}=v_{c\bar{c}}^{(l)}-\mathcal{M}_D$ versus the separation l.

obtain

$$L_0 e \geq 2[\pi/16+(m/e)^2]^{1/2}\ . \tag{6.3}$$

This is the dashed curve in Fig. 6. We see how close the data are with respect to that bound. It shows that the m/e dependence of the screening length is mostly contained in the factor m_D, since the data imply that

$$L_0 e \approx 2[\pi/16+(m/e)^2]^{1/2} \text{ at } m/e\to\infty\ ,$$

$$L_0 e \approx 3[\pi/16+(m/e)^2]^{1/2} \text{ at } m/e=0\ .$$

B. Gauss's law in action

By looking at the potential $V_{c\bar{c}}^{(L)}$ in Eq. (2.3), we distinguish two regimes, one characterized by $L \ll L_0$ where $V_{c\bar{c}}^{(L)}$ increases linearly, and the other where $L \gg L_0$, for which the potential is constant. It should be interesting to see how all this translates in terms of the electric field and the d-quark occupation number.

Fortunately, the EPMC algorithm allows for the computation of the expectation value of any operator σ diagonal in the basis $|e_n,N_n\rangle$. It is given by[23]

$$\langle 0|\sigma|0\rangle=\left\langle\frac{\langle\psi^{(n)}|\sigma|\psi^{(n)}\rangle}{\langle\psi^{(n)}|\psi^{(n)}\rangle}\right\rangle_n\ ,$$

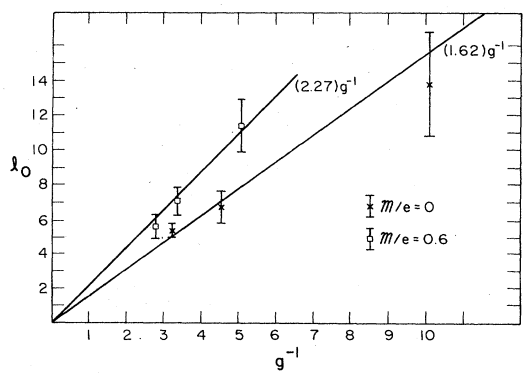

FIG. 4. The screening length l_0 (in lattice units) versus the coupling (g^{-1}). Both straight lines are fits, from which the continuum value is extracted.

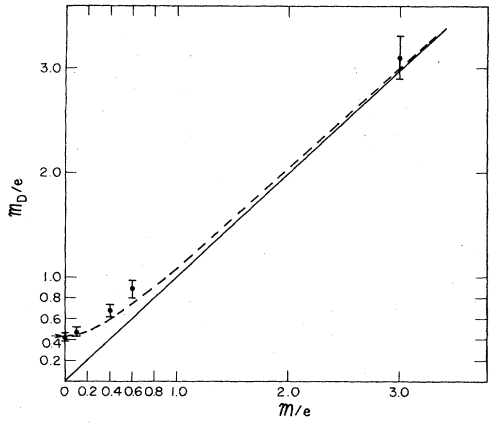

FIG. 5. The binding energy m_D/e versus the d-quark mass m/e. The solid and dashed lines represent, respectively, the high-m [Eq. (4.5)] and the MIT-bag-inspired [Eq. (6.1)] predictions. The arrow indicates the exact result at $m/e=0$.

for $n\rightarrow$ large (extra work is needed here, because the quantity $|\langle\psi^{(n)}|\{e_n,N_n\}\rangle|^2$ is a major ingredient and is not available in a straight energy calculation; for details see Ref. 23).

Since we are using Kogut-Susskind fermions, the dynamical fermions occupy two sites, instead of only one like the c quark. This will result in a "saw-tooth" oscillation of the electric field with respect to the lattice site. In order to remove this effect, we have chosen to compute the expectation value of a smoother expression for the electric field, i.e.,

$$\bar{E}_n^2\equiv(E_{n-2}^2+E_{n-1}^2+E_n^2+E_{n+1}^2+E_{n+2}^2)/5\ , \qquad (6.4)$$

which should be closer to the continuum $E_{(x)}^2$ anyway.

We have computed $\langle\bar{E}_n^2\rangle$ and $\langle N_n\rangle$ between the state $|\epsilon^{(l)}_{+1,-1}\rangle$, for $\mu/g=0$ with $g=0.31$, and $\mu/g=0.4$ with $g=0.4$; for both masses, $l=0,3,5,15$. Figures 7 and 8 show the $m/e=0.4$ case, where $l_0\simeq 5$.

By looking at $\langle\bar{E}_n^2\rangle$ first, one clearly sees the presence

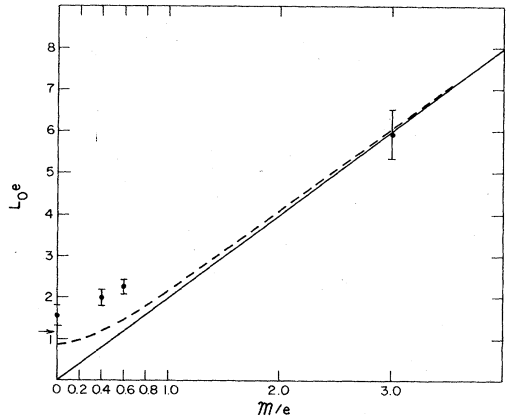

FIG. 6. The screening length eL_0, versus the d-quark mass. The solid and dashed lines represent, respectively, the high-m [Eq. (4.6)] prediction and the lower bound (6.3). The arrow shows the exact result at $m/e=0$.

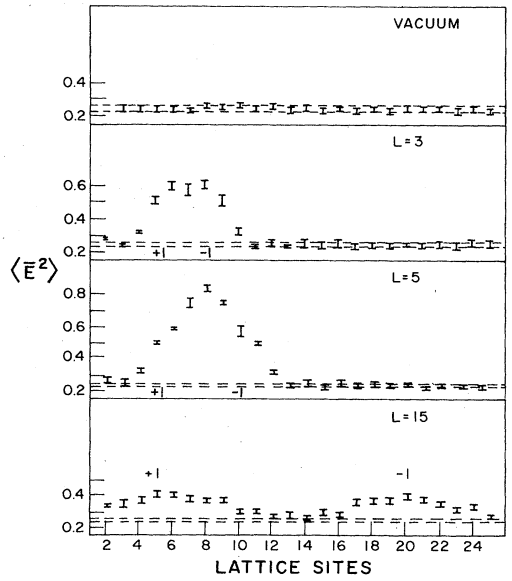

FIG. 7. The expectation value of the (averaged) square of the electric field $\langle\bar{E}^2\rangle$, versus the lattice sites. $m/e=0.4$, $g=0.4$; the screening length is $l_0=5\pm1$. The ±1 indicates the position of the sources.

of two distinct hadrons at a separation larger than the screening length ($l=15$). Inspection of $\langle N_n\rangle$ confirms this also. On the other hand, pair formation seems to be absent for $l<l_0$; it barely starts to show up at $l=l_0$. (This can be seen in the case $m/e=0$ also.)

From these observations we conclude that for $l<l_0$, the interaction between the sources is essentially mediated by the electric field. On the other hand, both electric field and pair creation are present at $l\gg l_0$, canceling the ef-

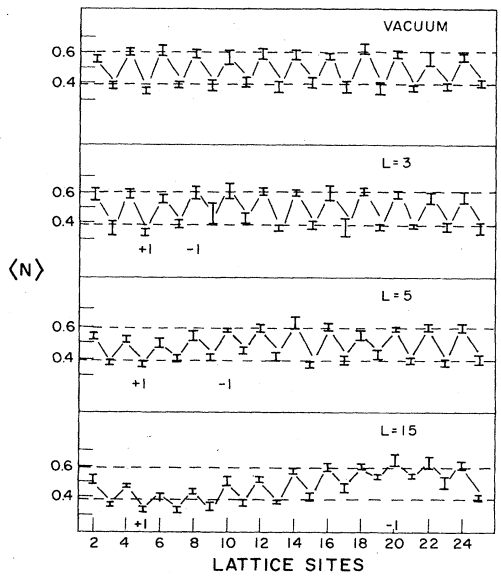

FIG. 8. The expectation value of the d-quark occupation number versus the lattice site. $m/e=0.4$, $g=0.4$; the screening length is $l_0=5\pm1$. The ±1 indicates the position of the sources.

fect of each other (screening). Unfortunately the data were not accurate enough to get a quantitative picture of all this.

Let us point out that the behavior of the quantity $\langle N_n \rangle$ seems to indicate the onset of pair production at $l \approx l_0$ ($l_0 = 5$ in Fig. 8). This observation together with the fact that the ratio $e^2 L_0 / m_D$ has a small but noticeable m/e dependence, confirms some of the physics we intended to represent in our definition of the screening length (i.e., the production of the first few pairs of d quarks involved in screening).

VII. CONCLUDING REMARKS

In a subsequent work, we will study screening phenomena in the Schwinger model with two flavors of dynamical fermions. It should be interesting to see the contribution of each flavor, especially when their masses are different. From the results obtained in this work we anticipate most of the flavor dependence to be contained in m_D; using MIT bag ideas, we could write

$$eL_0 \geq \frac{1}{eT_{(0)}} \left[\sum_{i=1}^{2} N_i [c_i + (m_i/e)^2]^{1/2} + B(m_1, m_2) \right] .$$

The definition of the screening length used throughout this work is general enough to be applied to several cases pertaining to the real world; charmonium systems come immediately to our mind.

It is now well known that charmonium and Υ bound states can be well described by the Schrödinger equation, with a potential $V_{c\bar{c}}^{(L)}$ given by[39]

$$V_{c\bar{c}}^{(L)} = -\frac{0.507}{L} + (0.17 \text{ GeV}^2) L . \tag{7.1}$$

The c and b quarks are heavy compared to the (constituent) masses of u, d, and s quarks ($m_u/m_c \approx m_d/m_c \approx 0.2$; $m_b/m_c \approx 3$). Presumably, we could use the ideas developed here to evaluate the screening length involved when charm (bottom) quarks are *adiabatically* separated from each other to form D mesons (B mesons).

The potential (7.1) is incomplete in the sense that it describes only the physics at short distances, i.e., $L < 4.0$ GeV^{-1}, so that $T_{(L_0)}$ is unknown. However, intuition suggests that, for longer distances, $V_{c\bar{c}}$ should increase monotonically with L, up to a point where it levels off (hadronization). This behavior should be such that $T_{(L_0)} \leq (0.17 \text{ GeV}^2)$, in which case

$$L_0 \geq m_{D,B} \frac{1}{(0.17 \text{ GeV}^2)} . \tag{7.2}$$

Here $m_{D,B}$ is the binding energy of the u and d quarks to the charmed one (or bottom) in $D(B)$ mesons. It is given by

$$m_D \simeq M_D - m_c \approx (1.9\text{—}1.4) \text{ GeV} \approx 0.5 \text{ GeV} ,$$

$$m_B \simeq M_B - m_b \approx (5.3\text{—}4.8) \text{ GeV} \approx 0.5 \text{ GeV} ,$$

so that

$$L_0^{D,B} \geq 2.9 \text{ GeV}^{-1} \simeq 0.58 \text{ fm} .$$

This lower bound is smaller, but close to the mean radii of the $c\bar{c}$ and $b\bar{b}$ states nearby the $D\bar{D}$ and $B\bar{B}$ threshold:[40]

$$R_{\psi'} \approx 0.85 \text{ fm} , \quad R_{\Upsilon'''} \approx 0.95 \text{ fm} .$$

The screening length derived from the condition $V_{(L_0)} = m_{D,B}$ seems to be realistic indeed.

ACKNOWLEDGMENTS

I would like to thank my thesis advisor, T. A. DeGrand, for suggesting this interesting problem, and for the enlightening discussions I had with him. Also, I would like to thank R. Ladbury, M. O'Callaghan, J. Smith, W. Wilcox, and R. M. Woloshyn for helpful suggestions. This work was supported by the Department of Energy.

[1] A more detailed description can be found in S. D. Ellis, in *Dynamics and Spectroscopy at High Energy,* proceedings of the 11th SLAC Summer Institute, 1983, edited by P. M. McDonough (SLAC, Stanford, 1984).

[2] B. Andersson, G. Gustafson, G. Ingelman, and T. Sjöstrand, Phys. Rep. **97**, 31 (1983).

[3] B. Andersson, G. Gustafson, and C. Peterson, Z. Phys. C **1**, 105 (1979).

[4] J. B. Kogut, Rev. Mod. Phys. **55**, 775 (1983).

[5] M. Creutz, *Quarks, Gluons and Lattices* (Cambridge University Press, Cambridge, 1983).

[6] B. Berg, CERN Report No. TH3978/84 (unpublished).

[7] C. Bernard, Phys. Lett. **108B**, 431 (1982); Nucl. Phys. **B219**, 341 (1983).

[8] H. G. Dosch and V. F. Müller, Nucl. Phys. **B158**, 419 (1979).

[9] T. A. DeGrand, in *Proceedings of the XIIIth International Symposium on Multiparticle Dynamics, Volendam, The Netherlands, 1982,* edited by W. Kittel, W. Metzger, and A. Stergiou (World Scientific, Singapore, 1983).

[10] The adiabatic approximation is an essential ingredient in the study of molecular collisions. See, for example, S. G. Christov, in *Collision Theory and Statistical Theory of Chemical Reactions,* Lecture Notes in Chemistry, Vol. 18 (Springer, Berlin, 1980).

[11] In principle the velocity of the sources, as well as the quantum nature of screening, could be reintroduced by considering the scattering with the other gluon-light-fermions states containing the *same* source distribution (the source separation may vary). The outline of such a scattering calculation should be similar to molecular collision theory (Ref. 10). Here, the sources would play the same role as the nucleus in the molecular case. This possibility is presently under investigation.

[12] D. Weingarten, Nucl. Phys. B (to be published).

[13] P. Becher, Ann. Phys. (N.Y.) **146**, 223 (1983).

[14] J. Schwinger, Phys. Rev. **128**, 2425 (1962); J. Lowenstein and A. Swieca, Ann. Phys. (N.Y.) **68**, 172 (1971).

[15]A. Casher, J. Kogut, and L. Susskind, Phys. Rev. D **10**, 732 (1974).
[16]S. Coleman, R. Jackiw, and L. Susskind, Ann. Phys. (N.Y.) **93**, 267 (1975).
[17]H. J. Rothe, K. D. Rothe, and J. A. Swieca, Phys. Rev. D **19**, 3020 (1979).
[18]A. Schiller and J. Ranft, Nucl. Phys. **B225** [FS9], 204 (1983); J. Ranft and A. Schiller, Phys. Lett. **112B**, 403 (1983).
[19]I. Bender, H. J. Rothe, and K. D. Rothe, Nucl. Phys. **B251** [FS13], 745 (1985).
[20]A. Duncan and M. Furman, Nucl. Phys. **B190** [FS3], 767 (1981); B. E. Baaquie, Phys. Rev. D **27**, 962 (1983).
[21]J. Ambjorn, P. Olesen, and C. Peterson, Nucl. Phys. **B240** [FS12], 189 (1984).
[22]D. K. Campbell, T. A. DeGrand, and S. Mazumdar, Phys. Rev. Lett. **52**, 1717 (1984); and (unpublished).
[23]T. A. DeGrand and J. Potvin, Phys. Rev. D **31**, 871 (1985).
[24]R. Blankenbecler and R. L. Sugar, Phys. Rev. D **27**, 1304 (1983).
[25]J. E. Hirsch, R. L. Sugar, D. J. Scalapino, and R. Blankenbecler, Phys. Rev. B **26**, 5033 (1982).
[26]D. M. Ceperley and M. M. Kalos, in *Monte Carlo Methods in Statistical Physics*, edited by K. Binder (Springer, New York, 1979).
[27]D. Heys and R. Stump, Phys. Rev. D **30**, 1315 (1984); M. A. Lee, K. A. Motakabbir, and K. E. Schmidt, Phys. Rev. Lett. **53**, 1191 (1984).
[28]S. Coleman, Ann. Phys. (N.Y.) **101**, 239 (1976).
[29]S. Coleman, Phys. Rev. D **11**, 2088 (1975).
[30]O. Martin and S. Otto, Nucl. Phys. **B203**, 297 (1982).
[31]H. W. Hamber, Phys. Rev. D **24**, 951 (1981).
[32]T. Banks, L. Susskind, and J. Kogut, Phys. Rev. D **13**, 1043 (1976); D. R. T. Jones, R. D. Kenway, J. B. Kogut, and D. K. Sinclair, Nucl. Phys. **B158**, 102 (1979).
[33]A. Carrol, J. Kogut, D. K. Sinclair, and L. Susskind, Phys. Rev. D **13**, 2270 (1976); **14**, 1729(E) (1976).
[34]R. D. Kenway and C. J. Hamer, Nucl. Phys. **B139**, 85 (1978), Appendix A.
[35]E. Marinari, G. Parisi, and C. Rebbi, Nucl. Phys. **B190** [FS3], 734 (1981).
[36]S. D. Drell, M. Weinstein, and S. Yankielowicz, Phys. Rev. D **14**, 1627 (1976); P. Nason, SLAC Report No. 3481, 1984 (unpublished); C. M. Bender, K. A. Milton, and D. H. Sharp, Phys. Rev. D **31**, 383 (1985).
[37]E. Lieb, T. Schultz, and D. Mattis, Ann. Phys. (N.Y.) **16**, 407 (1961).
[38]T. DeGrand, R. L. Jaffe, K. Johnson, and J. Kiskis, Phys. Rev. D **12**, 2060 (1975).
[39]C. Quigg and J. L. Rosner, Phys. Rep. **56**, 167 (1979).
[40]W. Buchmüller and S.-H. H. Tye, Phys. Rev. D **24**, 132 (1981).